Available online at www.sciencedirect.com
ScienceDirect
Journal of Sound and Vibration 312 (2008) 736–753
JOURNAL OF SOUND AND VIBRATION
www.elsevier.com/locate/jsvi

Dynamic behavior of multi-span bridges under moving loads with focusing on the effect of the coupling conditions between spans

Hongan Xu, Wen L. Li*

Department of Mechanical Engineering, Wayne State University, 5050 Anthony Wayne Drive, Detroit, MI 48202, USA

Received 27 March 2007; received in revised form 1 November 2007; accepted 7 November 2007
Available online 20 February 2008

Abstract

This study is concerned with the dynamic behavior of generic multi-span bridges under the action of moving loads. In this multi-span bridge model, each span can be independently supported by up to eight elastic springs, thus allowing a more general and realistic representation of many joints and intermediate supports of practical interest. Additionally, since the displacement and its first derivative are no longer required to be continuous at an intermediate support or at the junctions of spans, this model is capable of accounting for the possible steps and skew angles at these locations which are important to studying the vehicle–bridge interactions. Numerical results are presented with a focus on the dynamic impact of the coupling conditions between spans. It has been shown that the deflection on each span strongly depends upon its local coupling conditions, especially near the critical stiffness values. A fairly large variance of response has also been observed on each span in correspondence to a wide range of stiffness values, which implies a good potential for improving bridge performance through modifying joint parameters or coupling configurations. This model can be readily applied to any boundary and coupling conditions with no need of modifying the formulations or solution procedures.
© 2007 Elsevier Ltd. All rights reserved.

1. Introduction

The dynamic behavior of multi-span beams under moving loads has been extensively studied for many years in connection with the design of railway tracks and bridges. Although a grid-based solution method may be considered inconvenient in dealing with the problems involving moving loads, the finite element method is still one of the most powerful numerical methods and used by many researchers [1–3]. Dynamic stiffness method is another popular technique for the vibrations of beams subjected to moving loads [4–7]. Henchi and Fafard [4] derived the frequencies and mode shapes of a uniform continuous beam by using the dynamic stiffness element method under the framework of finite element approximation. Dugush and Eisenberger [7] presented a solution for the multi-span non-uniform beams transversed by a load traveling at a constant or variable velocity. The assumed mode method is also widely used to solve single- and multi-span beam problems [8–13].

*Corresponding author. Tel.: +1 313 577 3875.
E-mail address: wli@wayne.edu (W.L. Li).

0022-460X/$ - see front matter © 2007 Elsevier Ltd. All rights reserved.
doi:10.1016/j.jsv.2007.11.011

Ichikawa and Miyakawa [12] gave a solution for a uniform continuous beam under a concentrated load moving at variable velocity. The solution was based on the mode superposition method and the final system equations in the case of variable velocity were solved numerically using the central difference method. The vibration of a multi-span non-uniform beam was studied in Refs. [13,14] using the modified beam vibration functions as the assumed modes. Other commonly used methods include Laplace transformations [15–18], the methods of Lagrange multipliers [19–21], the Green's function methods [22–26], and so on.

In bridge design, elastic bearings are traditionally installed between bridge girders and the supporting structures to reduce the seismic forces or vibrations transmitted from the ground. However, in studying the dynamic responses of bridges to moving loads or vehicles, the end or intermediate supports have been mostly assumed to be ideal or homogeneous, implying that an adequate number of force or displacement components can be directly specified at these locations. Vibrations of bridges with elastic bearings were studied in Refs. [27,28] where the vibration shape of the beam was expressed as the superposition of the first modal shape of the flexural deflection of the beam with simple supports and the first modal shapes of a rigid beam supported by the elastic springs. It is shown that the elastic supports can have a meaningful impact on the dynamic response depending upon the vibration phases of the elastic bearings and the flexible beam [27]. The effects of boundary flexibility on the vibration of a beam was also studied in Ref. [29] by using eigenfunction expansion series, and it was found that the high-order modes would contribute significantly to the shear force calculations in the elastically supported case.

Many of the aforementioned methods will require a varying degree of modifications or adaptations to account for the variances in boundary conditions, intermediate supports, and/or the number of spans. For instance, when the unconstrained beam functions are used as the assume mode shapes, one typically needs to first determine the eigenfunctions for the given boundary conditions. This problem itself may become a sizeable task if the beam is elastically restrained at either or both ends. In addition, the beam eigenfunctions tend to become numerically unstable for large modal indexes, which demands special treatments in actual calculations.

In most investigations, the terms "multi-span bridges" or "multi-span beams" typically refer to a continuous beam with a number of intermediate supports. Although the beams may be allowed to have different physical or geometrical properties for each span, the beam displacement and its first derivatives are usually required to be continuous over the entire beam length. This condition can be easily violated when the translational and rotational couplings between any two adjacent spans are not sufficiently strong to ensure a smooth transition of the displacement and its derivative at the junction. Many modern structures such as bridges, railway tracks, and pipelines are assembled from some fundamental building blocks through joints. Thus, it is important to extend the definition of multi-span beam to include a beam system comprising a number of beams co-linearly coupled together via rigid and non-rigid joints. Accordingly, at the junctions the kinematic continuity requirements on the displacement functions will need to be replaced with the dynamic equilibrium equations about the forces and moments.

A modified Fourier series method was recently developed for determining the vibrations of a single beam with elastic boundary supports [30] and vibrations of two elastically coupled beams with/without an angle [31,32]. In this investigation, we will study the dynamic response of a multi-span bridge to a moving load with emphasizing on the effects of the between-span coupling conditions. Certain insightful information has been gained through numerical simulations regarding how to effectively modify the dynamic behavior of a multi-span bridge.

2. Description of the analysis method

Fig. 1 shows a multi-span bridge model which consists of any number of beams or spans coupled together via joints represented by linear and rotational springs. The elastic springs between any two adjacent beams allows considering the flexibility of some joints in practice such as bolts or point welds. The conventional rigid connectors can be considered as a special case when the stiffnesses of these springs become substantially larger than the bending rigidities of the beams. Each of beams may also be supported on a set of elastic restraints at both ends. All the traditional intermediate supports and homogeneous boundary conditions (i.e., the combinations of the simply supported, free, guided and clamped end conditions) can be readily obtained from

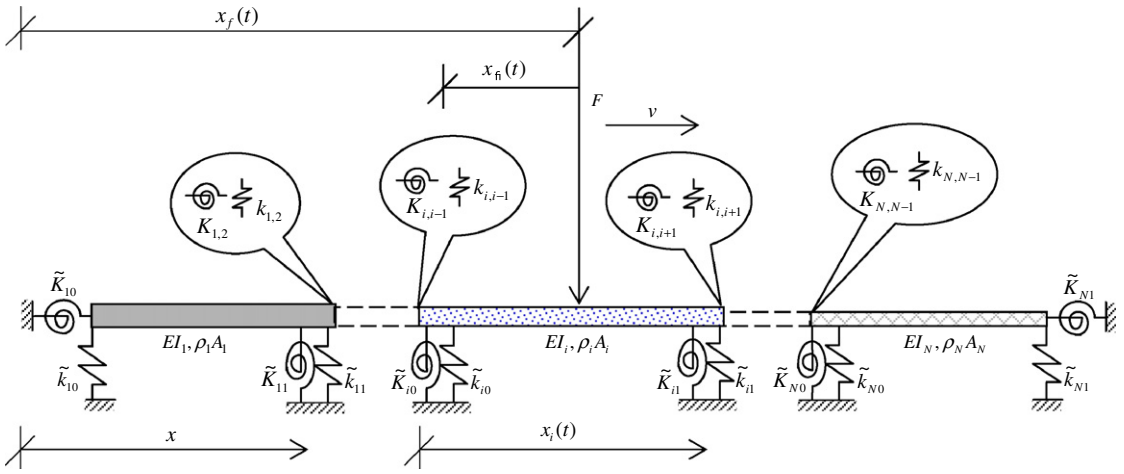

Fig. 1. A multi-span bridge subjected to a concentrated moving load.

these general boundary conditions by accordingly setting the stiffness constants of the restraining springs to equal to zero or infinity.

The differential equation for the vibration of the ith beam is well known as

$$D_i \partial^4 w_i(x,t)/\partial x^4 - \rho_i A_i \partial^2 w_i(x,t)/\partial t^2 = \sum_{j=1}^{J} F_j \delta\left(x - x_{j,i}^f(t)\right) \quad (i = 1, 2, \ldots, N), \tag{1}$$

where $w_i(x,t)$, D_i, ρ_i, and S_i are, respectively, the flexural displacement, the bending rigidity, the mass density and the cross-sectional area of ith beam; ω is angular frequency and x represents the local coordinate starting from the left end of the ith span; and J is the number of loads acting on the ith beam at t moment, F_j is the magnitude of the jth load, δ is the Dirac delta function, and $x_{j,i}^f(t)$ is the jth load position measured from the left end of the ith beam. Sometimes, unit step functions are used in Eq. (1) to explicitly specify whether a moving load is present to a span or not. For simplicity, they are not included in Eq. (1) since the load position described in terms of the delta function has already contained this information, i.e., the jth load is not present to the ith beam if $x_{j,i}^f(t) > L_i$ or < 0.

When a single load travels along a beam, the dynamic response can be treated as having two parts: the forced vibration caused by the load directly acting on the beam, and the residual free vibration caused by the load that has passed the beam [28]. As a consequence, phenomena of resonance and cancellation may occur when a bridge is under the action of multiple loads [27,28]. Therefore, the loading conditions (e.g., the number of loads and their traveling speeds) are of critical importance to a bridge design. From mathematical point of view, however, Eq. (1) simply represents a linear system whose response to multiple loads can be actually considered as the superposition of its responses to each individual load. Thus, only one moving force will be explicitly considered in this study since our primary objective is to examine if and how the coupling conditions between spans can affect the bridge vibration.

The load profile is defined by $\ddot{x}_f(t) = a = \text{const.}$, $\dot{x}_f(t) = v = v_0 + at$ and $x_f(t) = v_0 t + at^2/2$, where $x_f(t)$ is the load position measured from the left end of the first beam, a is the acceleration of the moving load, $v = v(t)$ is its velocity, and v_0 is the initial velocity at time $t = 0$ when the load is just about to enter the first beam.

The boundary and coupling conditions for the ith beam can be expressed in the following manner:

At $x = 0$,

$$k_{i,i-1}(w_i(0,t) - w_{i-1}(L_{i-1},t)) + \tilde{k}_{i0} w_i(0,t) = -D_i w_i'''(0,t), \tag{2}$$

$$K_{i,i-1}(w_i'(0,t) - w_{i-1}'(L_{i-1},t)) + \tilde{K}_{i0} w_i'(0,t) = D_i w_i''(0,t). \tag{3}$$

At $x = L_i$,

$$k_{i,i+1}(w_i(L_i,t) - w_{i+1}(0,t)) + \tilde{k}_{i1} w_i(L_i,t) = D_i w_i'''(L_i,t), \tag{4}$$

$$K_{i,i+1}(w_i'(L_i,t) - w_{i+1}'(0,t)) + \tilde{K}_{i1} w_i'(L_i,t) = -D_i w_i''(L_i,t). \tag{5}$$

At the left end (of the first beam),

$$\tilde{k}_{10} w_1(0,t) = -D_1 w_1'''(0,t), \tag{6}$$

$$\tilde{K}_{10} w_1'(0,t) = D_1 w_1''(0,t). \tag{7}$$

At the right end (of the Nth beam),

$$\tilde{k}_{N1} w_N(L_N,t) = D_N w_N'''(L_N,t), \tag{8}$$

$$\tilde{K}_{N1} w_N'(L_N,t) = -D_N w_N''(L_N,t), \tag{9}$$

where refer to Fig. 1, $k_{i,j}$ and $K_{i,j}$ denote the stiffnesses of the linear and rotational springs at the junction of beams i and j, respectively; $\tilde{k}_{i,0}, \tilde{k}_{i,1}$ are the stiffnesses of linear springs, and $\tilde{K}_{i,0}, \tilde{K}_{i,1}$ the stiffnesses of the rotational springs at the left and right ends of beam i, respectively.

All the conventional (homogeneous) beam boundary conditions can be considered as the special cases of Eqs. (6)–(9). For example, the simply supported end condition is easily modeled by simply setting the stiffnesses of the translational and rotational springs to be infinity and zero, respectively.

On each beam, the displacement will be sought in the form of

$$w_i(x,t) = \sum_{m=0}^{\infty} A_{i,m}(t) \cos\, \lambda_{i,m} x + p_i(x,t), \quad 0 \leqslant x \leqslant L_i \quad \left(\lambda_{i,m} = \frac{m\pi}{L_i}\right), \tag{10}$$

where L_i is the length of ith beam.

In Eq. (10), an auxiliary function $p_i(x)$ was introduced to improve the accuracy and convergence of the series expansion at the end points, $x = 0$ and L_i. It is specifically required to satisfy the following conditions:

$$p_i'''(0,t) = w_i'''(0,t) = \alpha_{i0}, \tag{11}$$

$$p_i'''(L_i,t) = w_i'''(L_i,t) = \alpha_{i1}, \tag{12}$$

$$p_i'(0,t) = w_i'(0,t) = \beta_{i0}, \tag{13}$$

$$p_i'(L_i,t) = w_i'(L_i,t) = \beta_{i1}. \tag{14}$$

The benefits for using such an auxiliary function were adequately discussed before in Ref. [30] and will not be further elaborated here. Theoretically, the auxiliary function $p_i(x)$ can be any continuous closed-form function defined over $[0, L_i]$. As an example, the auxiliary function $p_i(x)$ will be here selected as a polynomial:

$$p_i = \zeta_i(x)^{\mathrm{T}} \boldsymbol{\alpha}_i, \tag{15}$$

where

$$\boldsymbol{\alpha}_i = \{\alpha_{i0}, \alpha_{i1}, \beta_{i0}, \beta_{i1}\}^{\mathrm{T}} \tag{16}$$

and

$$\zeta_i(x)^{\mathrm{T}} = \begin{Bmatrix} -(15x^4 - 60L_i x^3 + 60L_i^2 x^2 - 8L_i^4)/360L_i \\ (15x^4 - 30L_i^2 x^2 + 7L_i^4)/360L_i \\ (6L_i x - 2L_i^2 - 3x^2)/6L_i \\ (3x^2 - L_i^2)/6L_i \end{Bmatrix}. \tag{17}$$

It should be pointed out that although the same symbol is used, the x-coordinate in Eq. (17) actually represents a local coordinate system with its origin at the left end of each beam. However, the use of different local coordinate systems is simply for the sake of mathematical convenience.

At this point, the auxiliary function is fully defined in terms of four unknown boundary constants, $\boldsymbol{\alpha}_i = \{\alpha_{i0}, \alpha_{i1}, \beta_{i0}, \beta_{i1}\}^{\mathrm{T}}$. In what follows, these unknowns will be determined as the functions of the Fourier coefficients.

Substituting Eqs. (10)–(17) into (2)–(9) leads to

$$k_{i,i-1}\left(\sum_{m=0}^{\infty}(-1)^m A_{i-1,m}(t) - \frac{7L_{i-1}^3\alpha_{i-1,0}}{360} - \frac{8L_{i-1}^3\alpha_{i-1,1}}{360} + \frac{\beta_{i-1,0}L_{i-1}}{6} + \frac{\beta_{i-1,1}L_{i-1}}{3}\right)$$
$$= D_i\alpha_{i,0} + (k_{i,i-1} + \tilde{k}_{i0})\left(\sum_{m=0}^{\infty} A_{i,m}(t) + \frac{8L_i^3\alpha_{i,0}}{360} + \frac{7L_i^3\alpha_{i,1}}{360} - \frac{\beta_{i,0}L_i}{3} - \frac{\beta_{i,1}L_i}{6}\right), \tag{18}$$

$$(K_{i,i-1} + \tilde{K}_{i0})\beta_{i,0} = K_{i,i-1}\beta_{i-1,1} + D_i\left(-\sum_{m=1}^{\infty}\lambda_{i,m}^2 A_{i,m}(t) - \frac{\alpha_{i,0}L_i}{3} - \frac{\alpha_{i,1}L_i}{6} + \frac{\beta_{i,1}}{L_i} - \frac{\beta_{i,0}}{L_i}\right), \tag{19}$$

$$(k_{i,i+1} + \tilde{k}_{i1})\left(\sum_{m=0}^{\infty}(-1)^m A_{i,m}(t) - \frac{7L_i^3\alpha_{i,0}}{360} - \frac{8L_i^3\alpha_{i,1}}{360} + \frac{\beta_{i,0}L_i}{6} + \frac{\beta_{i,1}L_i}{3}\right)$$
$$= D_i\alpha_{i,1} + k_{i,i+1}\left(\sum_{m=0}^{\infty} A_{i+1,m}(t) + \frac{8L_{i+1}^3\alpha_{i+1,0}}{360} + \frac{7L_{i+1}^3\alpha_{i+1,1}}{360} - \frac{\beta_{i+1,0}L_{i+1}}{3} - \frac{\beta_{i+1,1}L_{i+1}}{6}\right), \tag{20}$$

$$(K_{i,i+1} + \tilde{K}_{i1})\beta_{i,1} = K_{i,i+1}\beta_{i+1,0} - D_i\left(\sum_{m=1}^{\infty}(-1)^{m+1}\lambda_{i,m}^2 A_{i,m}(t) + \frac{\alpha_{i,0}L_i}{6} + \frac{\alpha_{i,1}L_i}{3} + \frac{\beta_{i,1}}{L_i} - \frac{\beta_{i,0}}{L_i}\right). \tag{21}$$

In matrix form, the above equations can be reduced to

$$\mathbf{H}_{i,i-1}\boldsymbol{\alpha}_{i-1} + \mathbf{H}_{i,i}\boldsymbol{\alpha}_i + \mathbf{H}_{i,i+1}\boldsymbol{\alpha}_{i+1} = \sum_{m=0}^{\infty}\left(\mathbf{Q}_{i,i-1}^m A_{i-1,m}(t) + \mathbf{Q}_{i,i}^m A_{i,m}(t) + \mathbf{Q}_{i,i+1}^m A_{i+1,m}(t)\right). \tag{22}$$

The definition of matrix $\mathbf{H}_{i,i-1}$, $\mathbf{H}_{i,j}$, $\mathbf{H}_{i,i+1}$ and vectors $\mathbf{Q}_{i,i-1}^m, \mathbf{Q}_{i,i}^m, \mathbf{Q}_{i,i+1}^m$ can be found in Ref. [33]. Eq. (22) contains four linear algebraic equations that relate the 12 boundary unknowns to the Fourier expansion coefficients. To determine the boundary unknowns, one has to apply Eq. (22), in turn, to each beam, resulting in a total of $4N$ equations [33]:

$$\overline{\mathbf{H}}\bar{\boldsymbol{\alpha}} = \sum_{m=0}^{\infty}\overline{\mathbf{Q}}^m\mathbf{A}_m \quad \text{or} \quad \bar{\boldsymbol{\alpha}} = \sum_{m=0}^{\infty}\widetilde{\mathbf{H}}\overline{\mathbf{Q}}^m\mathbf{A}_m. \tag{23}$$

Making use of Eqs. (15) and (23), Eq. (10) can be expressed as

$$w_i(x,t) = \sum_{m=0}^{\infty} A_{i,m}(t)(\cos\,\lambda_{i,m}x + \zeta_i(x)^{\mathrm{T}}\tilde{H}_i\bar{Q}_i^m) + \sum_{\substack{j=1,N\\ j\neq i}}\sum_{m=0}^{\infty} A_{j,m}(t)\zeta_j(x)^{\mathrm{T}}\tilde{H}_i\bar{Q}_j^m. \tag{24}$$

It should be noted that the boundary and coupling conditions, Eqs. (2)–(9), have been explicitly used in establishing the relationship between the boundary constants (in the polynomials) and the Fourier expansion coefficients. Thus, the Fourier coefficients are now only required to satisfy the governing differential equation.

Substituting Eq. (24) into Eq. (1) and following the standard Galerkin procedure, one is able to obtain

$$[\mathbf{K}_{ij}]\{\mathbf{A}_j\} + [\mathbf{M}_{ij}]\{\ddot{\mathbf{A}}_j\} = \{\mathbf{F}_i\} \quad (i,j = 1,2,3,\ldots,N), \tag{25}$$

where

$$K_{ij,mm'} = \delta_{ij}(1-\delta_{0m})(1-\delta_{0m'})(\delta_{mm'} + S_{i,m'm}^{ij})\lambda_{im'}^4 + \delta_{ij}\delta_{0m'}\delta_{m0}S_{i,00}^{ij} + (1-\delta_{ij})\delta_{m0}S_{i,0m'}^{ij}, \tag{26}$$

$$M_{ij,mm'} = \delta_{ij}(1-\delta_{0m})(1-\delta_{0m'})(\delta_{mm'} + S^{ij}_{i,mm'} + S^{ij}_{i,m'm} + Z^{ij}_{i,mm'}) + \delta_{ij}\delta_{0m'}\delta_{m0}(2 + Z^{ij}_{i,00}) + \delta_{ij}\delta_{0m'}(S^{ij}_{i,m0} + Z^{ij}_{i,m0}) + \delta_{ij}\delta_{m0}(S^{ij}_{i,m'0} + Z^{ij}_{i,m'0}) + (1-\delta_{ij})(1-\delta_{0m})(S^{ij}_{i,mm'} + Z^{ij}_{i,mm'}) + (1-\delta_{ij})\delta_{m0}Z^{ij}_{i,0m'} \quad (27)$$

and

$$f_{i,m} = 2/L_i \int_0^{L_i} \left(\cos\,\lambda_{im}x + \zeta_i(x)^{\mathrm{T}}\tilde{\mathbf{H}}_i\tilde{\mathbf{Q}}_i^m\right)F_1\left(x - x^f_{1,i}(t)\right)\mathrm{d}x \quad \text{for } m,m' = 0,1,2,3,\ldots, \text{ and } i,j = 1,2,3,\ldots,N. \quad (28)$$

The readers should refer to Ref. [33] for the definitions of matrices $S^{ij}_{i,mm'}$ and $Z^{ij}_{i,mm'}$ in the above equations. Eq. (25) represents a set of coupled second-order differential equations with respect to time which can be solved by direct numerical integration. In this study, the Newmark-β algorithm is used to perform the numerical integration.

3. Results and discussions

In order to validate the current model and analysis code, we will first consider a multi-span beam problem that was previously studied in Ref. [4]. As illustrated in Fig. 2, this example involves a three-span stepped beam subjected to a single concentrated moving load. The relevant beam and material parameters are listed in Table 1. Under the current framework, this stepped continuous beam can be viewed as a collection of three separate beams that are rigidly coupled together. The continuous beam is assumed to be simply supported at its ends and at the two joint locations. The simply supported condition can be readily modeled by simply setting the stiffnesses of the (linear and rotational) coupling springs equal to infinity and zero, respectively. In all the following calculations, the Fourier series for each beam is numerically truncated to include only first 10 terms.

The calculated natural frequencies for the first six modes are compared in Table 2 with those previously given in Ref. [4]. The mode shapes of first three modes are plotted in Fig. 3. Now, assume the beam is subjected to a point load, $F = 9.48 \times 10^3$ N, moving at a constant speed $v = 35.57$ m/s. Plotted in Fig. 4 are the

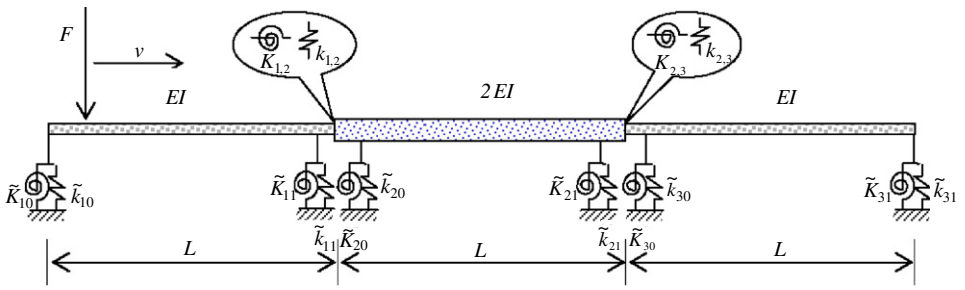

Fig. 2. A three-span beam with non-uniform cross-section under a moving load.

Table 1
Beam and material properties

Parameters	Values
L (m)	20
ρ (kg/m^3)	7800
ρA (kg/m)	1000
EI (N m^2)	1.96×10^9
E (N/m^2)	10.48×10^{10}
F (N)	9.48×10^3

Table 2
Comparison of natural frequencies

Mode	Current method (Hz)	Results from Ref. [4] (Hz)
1	6.195	6.204
2	7.579	7.581
3	11.795	11.974
4	24.095	24.207
5	26.365	26.439
6	37.561	37.282

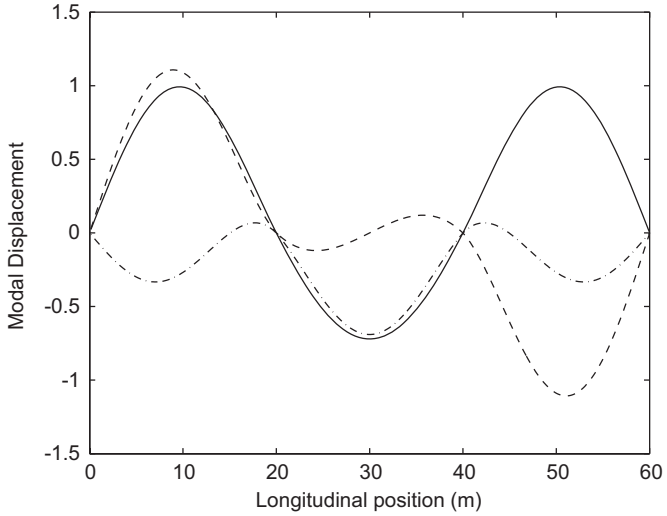

Fig. 3. Mode shapes for the first three modes of the three-span beam: (—) first, (- - -) second and (- · -) third.

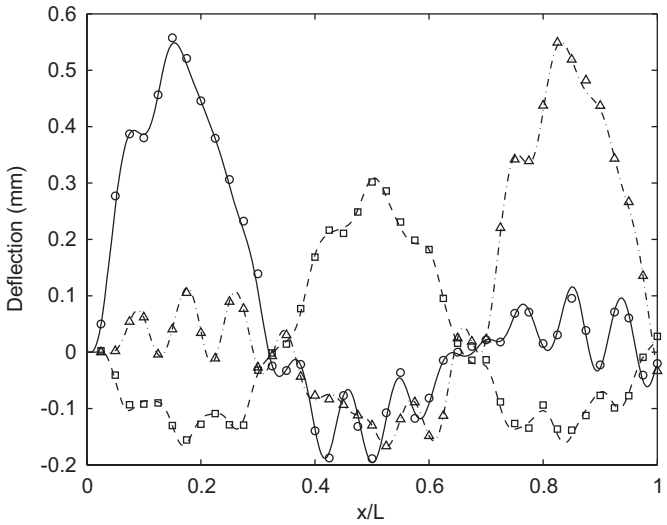

Fig. 4. Flexural deflection at the midpoint of each span for $v = 35.57$ m/s: span 1: (—) current, (○) [4]; span 2: (- - -) current, (□) [4]; and span 3: (- · -) current, (Δ) [4].

corresponding deflections at the midpoint locations of all three spans. The results obtained by Henchi and Fafard [4] are also shown there for comparison. An excellent agreement is observed between these two sets of solutions. This problem was also studied by Dugush and Eisenberger [7] for different beam

parameters and load profiles. It suffices to say that the current results also match closely with those given in Ref. [7].

Before proceeding to examination of the elastic couplings between spans, we will first consider a modified version of the above problem which involves a single uniform beam elastically supported at its ends. This kind of problems was previously investigated in Refs. [27–29]. For convenience, all the related parameters will remain the same except that the bending stiffness for the mid-span is reduced to EI, same as the other spans to achieve the uniformity required for a single-span beam. It should be mentioned that the two intermediate supports are also removed. Thus, we now deal with a uniform beam of length $3L$ elastically supported, at each end, by a linear spring of stiffness, say, $k = 10^{10}$ N/m. The deflections at the center of the beam are plotted in Fig. 5 for two different load speeds. The results obtained using the solution given by Yang et al. [27] are also presented there. A good comparison is observed between these two sets of results.

In a traditional multi-span beam problem, the beam displacement and its first derivative are both required to be continuous over the entire beam length. In many real-world applications, regardless of whether purposely or not, the joints between different spans may not always be modeled as being infinitely rigid. Thus, joint stiffnesses, or coupling conditions between spans, will actually constitute an additional set of model parameters, and may meaningfully affect the bridge vibration. While the roles of beam parameters and/or loading conditions have been extensively studied, the effect of the between-span coupling conditions on the dynamic behavior of a bridge was barely attempted before. Thus, the subsequent discussions will be primarily focused on the effect of the coupling conditions.

As illustrated in Fig. 2, there are up to eight independent springs associated with each span in a general support/coupling configuration. Theoretically, each of these springs can be considered as an independent design variable, which makes it a formidable task to study a general case involving an arbitrary combination of these variables. For simplicity, we will again consider the three-span beam problem with only one modification: the continuity requirement for the first derivative is relaxed at the junctions of the spans. That is, two rotational springs, $K_{1,2} = K_{2,3} = K$, of equal stiffness are now placed between the spans while the displacement is still assumed to be continuous over the entire length. Three different arrangements are considered: (1) spans 1 and 2 are elastically connected via a rotational spring while spans 2 and 3 are rigidly coupled together (ER); (2) spans 2 and 3 are elastically connected while spans 1 and 2 are rigidly coupled together (RE); and (3) all three spans are elastically coupled together (EE). In all these cases, the rotational stiffness will vary from 10^6 to 10^{10} N m/rad.

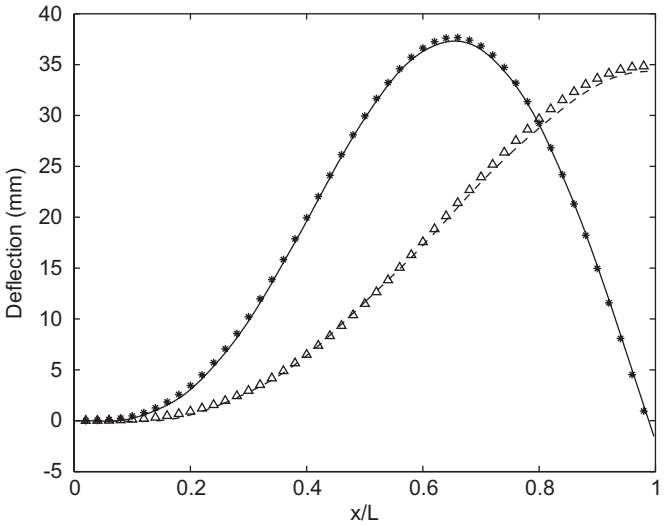

Fig. 5. Flexural deflection at the midpoint of a continuous elastically supported beam under a load with two different velocities: $v = 35.57$ m/s: (—) current method, (*) [27]; and $v = 71.25$ m/s: (- - -) current method, (Δ) [27].

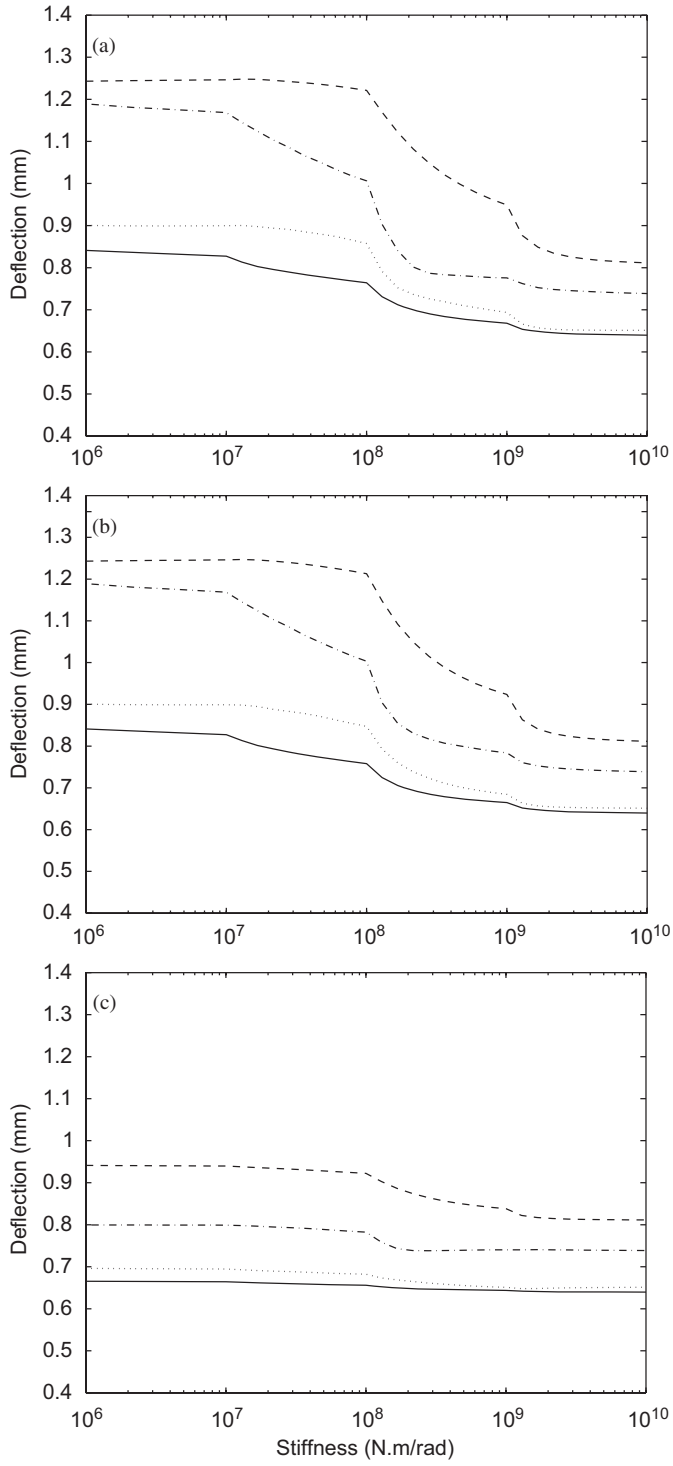

Fig. 6. Peak–peak deflection at the midpoint of the first span for a few load profiles defined by a constant acceleration $a = 2\,\mathrm{m/s^2}$ and different initial velocities: (a) elastic–elastic; (b) elastic–rigid; and (c) rigid–elastic. (—) $v = 5\,\mathrm{m/s}$, (· · · · ·) $v = 17.87\,\mathrm{m/s}$, (- - -) $v = 35.57\,\mathrm{m/s}$, and (- - -) $v = 71.25\,\mathrm{m/s}$.

The peak–peak value (the algebraic difference between the extremes of the deflection) at the midpoint of each span is utilized to evaluate the dynamic behavior of the beam system. Figs. 6–8 show the peak–peak values vs. the stiffness of the coupling springs for a few different load profiles. It is seen that as the stiffness increases, the

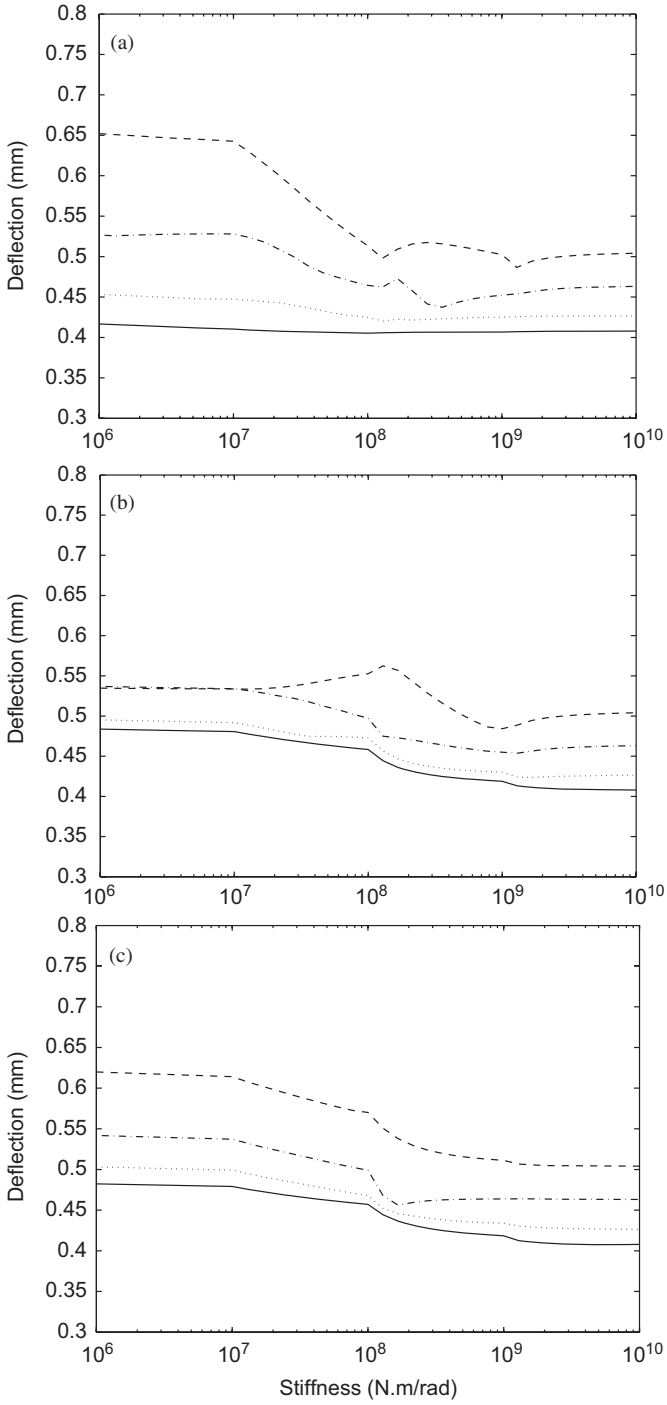

Fig. 7. Peak–peak deflection at the midpoint of the second span for a few load profiles defined by a constant acceleration $a = 2\,\mathrm{m/s^2}$ and different initial velocities: (a) elastic–elastic; (b) elastic–rigid; and (c) rigid–elastic. (—) $v = 5\,\mathrm{m/s}$, (· · · · ·) $v = 17.87\,\mathrm{m/s}$, (- · -) $v = 35.57\,\mathrm{m/s}$, and (- - -) $v = 71.25\,\mathrm{m/s}$.

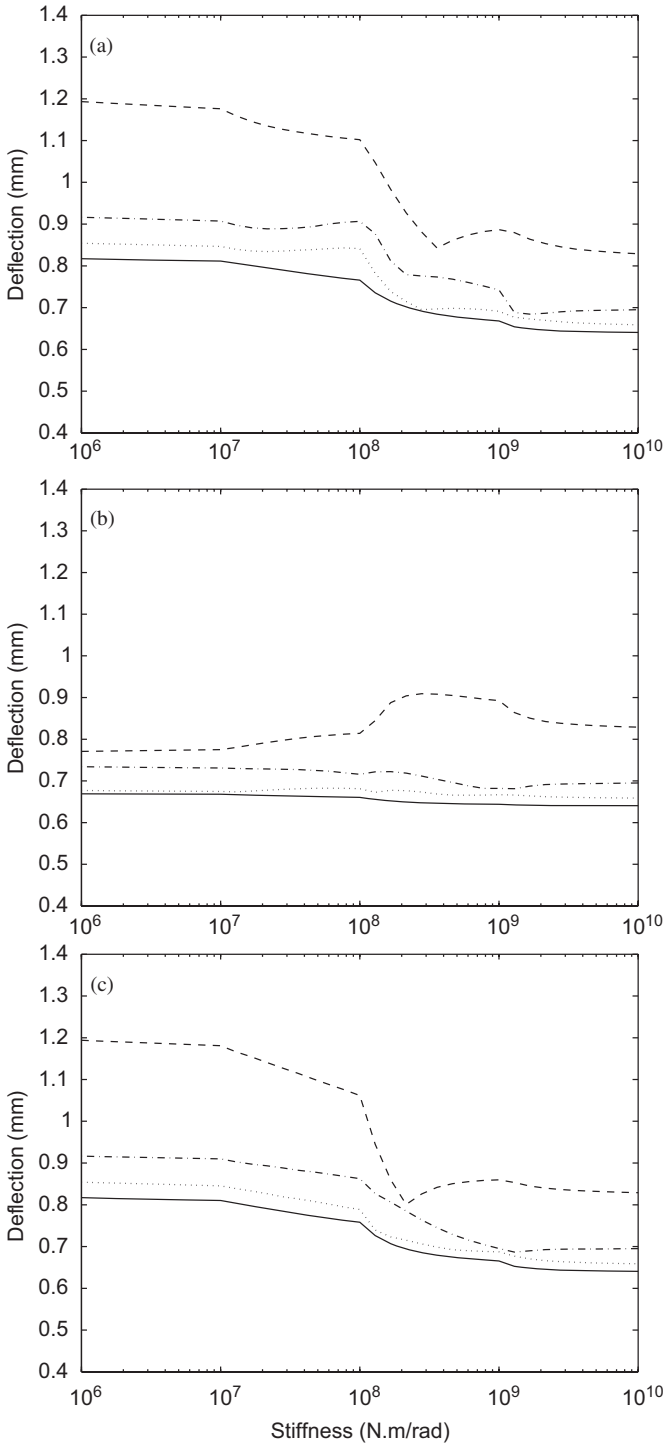

Fig. 8. Peak–peak deflection at the midpoint of the third span for a few load profiles defined by a constant acceleration $a = 2\,\mathrm{m/s^2}$ and different initial velocities: (a) elastic–elastic; (b) elastic–rigid; and (c) rigid–elastic. (—) $v = 5\,\mathrm{m/s}$; (· · · · ·) $v = 17.87\,\mathrm{m/s}$; (- - -) $v = 35.57\,\mathrm{m/s}$; and (- - -) $v = 71.25\,\mathrm{m/s}$.

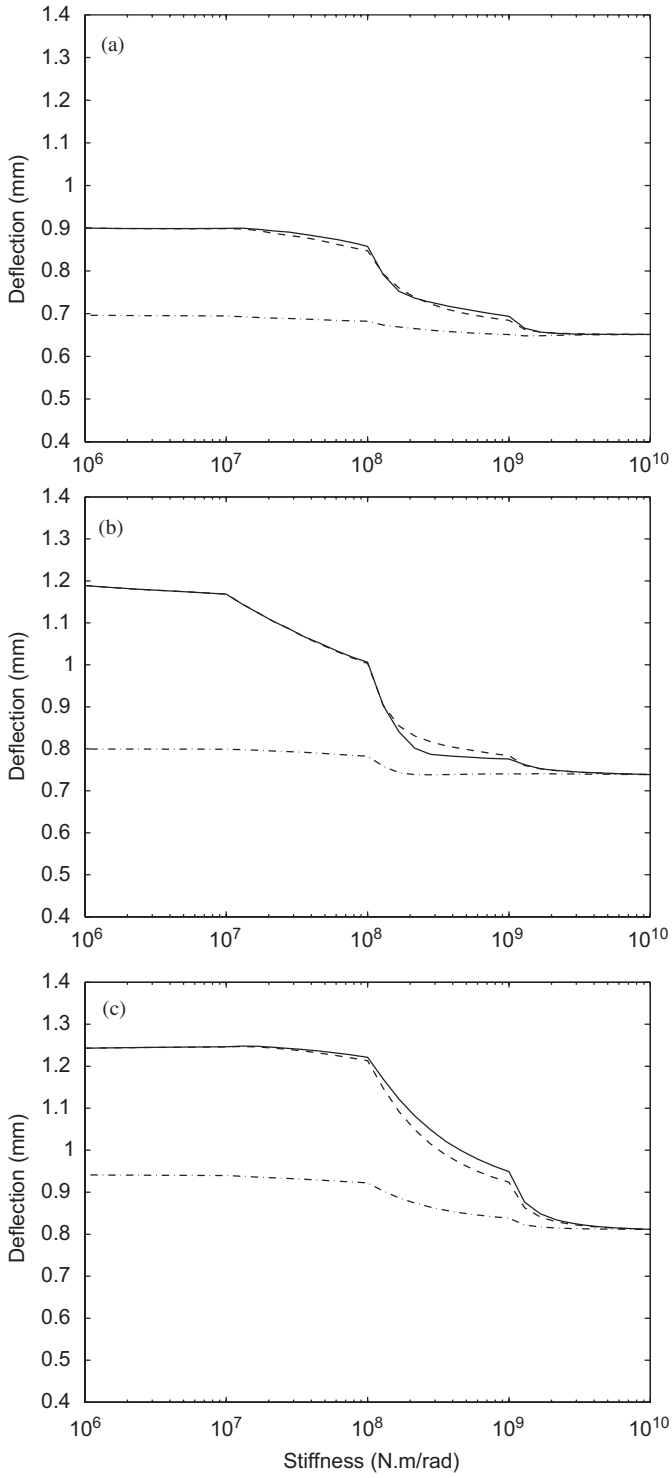

Fig. 9. Peak–peak deflection at the midpoint of the first span for a constant acceleration $a = 2\,\mathrm{m/s^2}$: (a) $v = 17.87\,\mathrm{m/s}$; (b) $v = 35.57\,\mathrm{m/s}$; and (c) $v = 71.25\,\mathrm{m/s}$. (—) Elastic–elastic; (- - -) elastic–rigid; and (- · -) rigid–elastic.

deflection at the midpoint of each span typically decreases until $K \cong 10^8$ (or $KL/EI \cong 1$). The dynamic responses tend to exhibit a strong dependence on the coupling stiffness near this "critical" value. The peak–peak values typically increases with the traveling speed of the load for a given coupling stiffness and configuration.

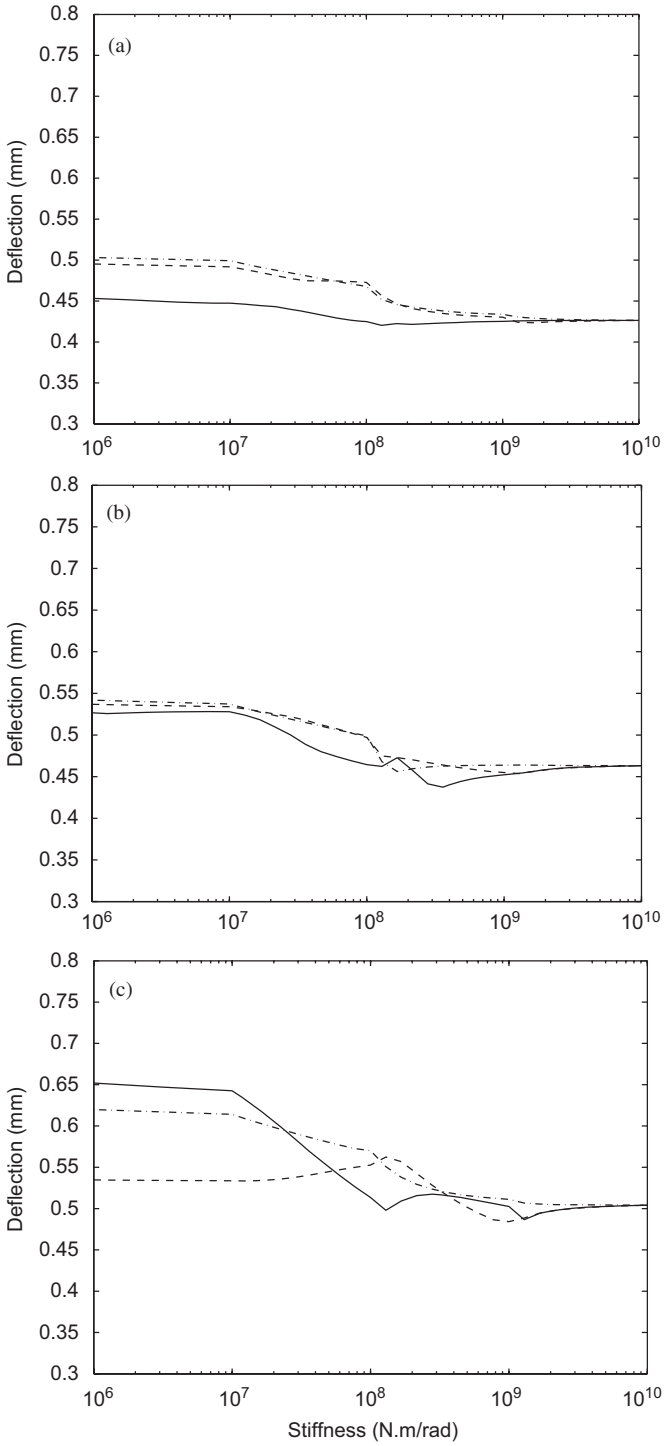

Fig. 10. Peak–peak deflection at the midpoint of the second span for a constant acceleration $a = 2\,\mathrm{m/s^2}$: (a) $v = 17.87\,\mathrm{m/s}$; (b) $v = 35.57\,\mathrm{m/s}$; and (c) $v = 71.25\,\mathrm{m/s}$. (—) Elastic–elastic; (- - -) elastic–rigid; and (- · -) rigid–elastic.

To better understand the effect of coupling conditions, the results in Figs. 6–8 are re-plotted in Figs. 9–11 based on the coupling configurations. It is observed that the deflections on span 1 are almost the same for the EE and ER configurations. A possible explanation is that the peak deflections

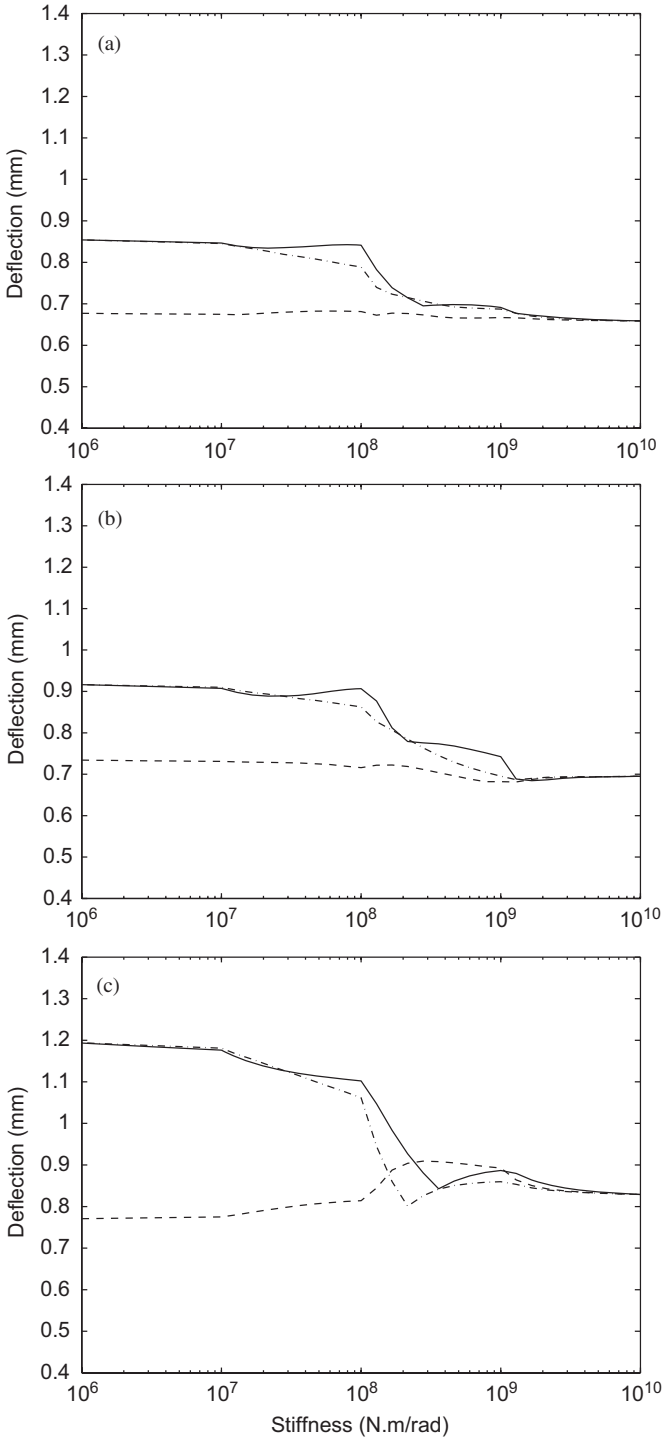

Fig. 11. Peak–peak deflection at the midpoint of the third span for a constant acceleration $a = 2\,\mathrm{m/s^2}$: (a) $v = 17.87\,\mathrm{m/s}$; (b) $v = 35.57\,\mathrm{m/s}$; and (c) $v = 71.25\,\mathrm{m/s}$. (—) Elastic–elastic; (- - -) elastic–rigid; and (- · -) rigid–elastic.

occur when the load is still located on the first span. Since the time elapsed to reach this stage is relatively short, the wavefront may not yet have arrived at or bounced back from the junction (between spans 2 and 3) which differentiates the EE and ER configurations. As a consequence, the initial response of

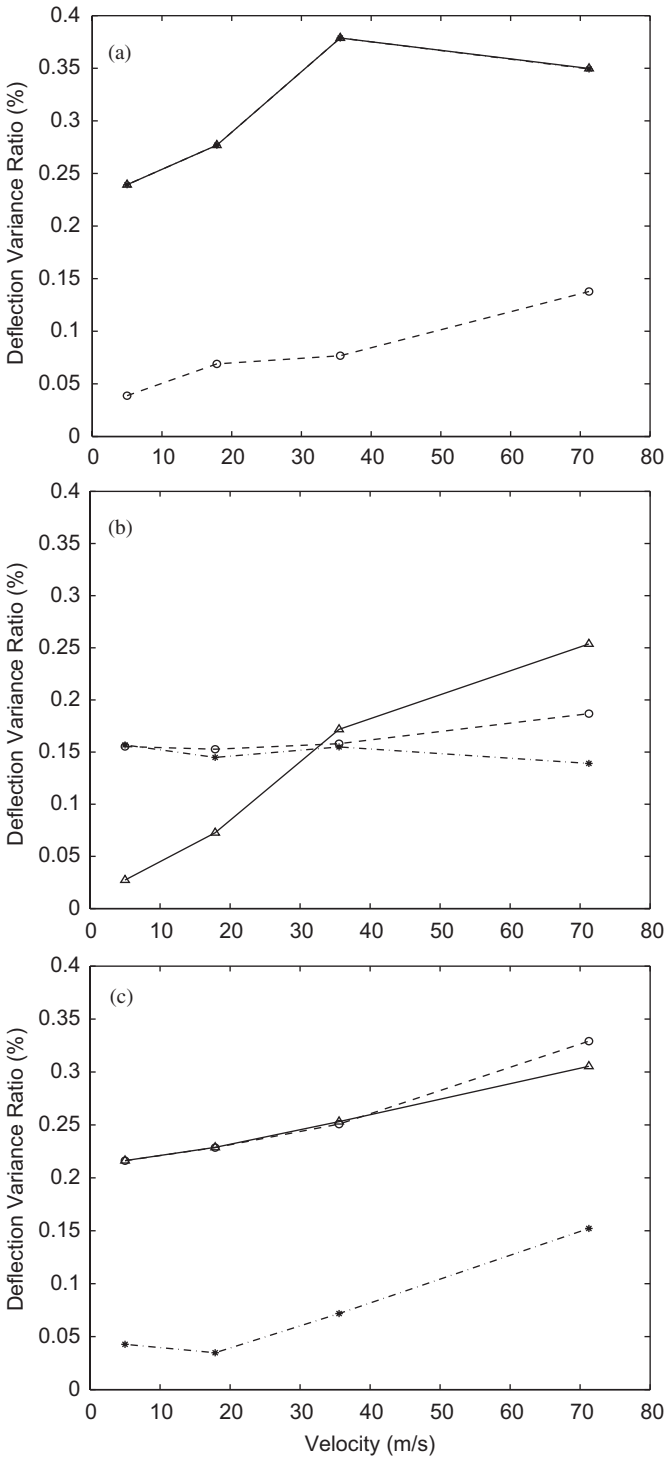

Fig. 12. Variation ratio for the peak–peak deflection at the midpoint of each span for a constant acceleration $a = 2\,\mathrm{m/s^2}$: (a) span 1; (b) span 2; and (c) span 3. (—△—) Elastic–elastic; (- -○- -) rigid–elastic; and (—*— -) elastic–rigid.

span 1 is primarily dictated by the local end conditions which are essentially the same in both configurations. A similar comparison can be made between the EE and RE configurations regarding the deflections on span 3 for $K \leqslant 10^7$. As the spring stiffness becomes sufficiently large, all the three configurations will essentially

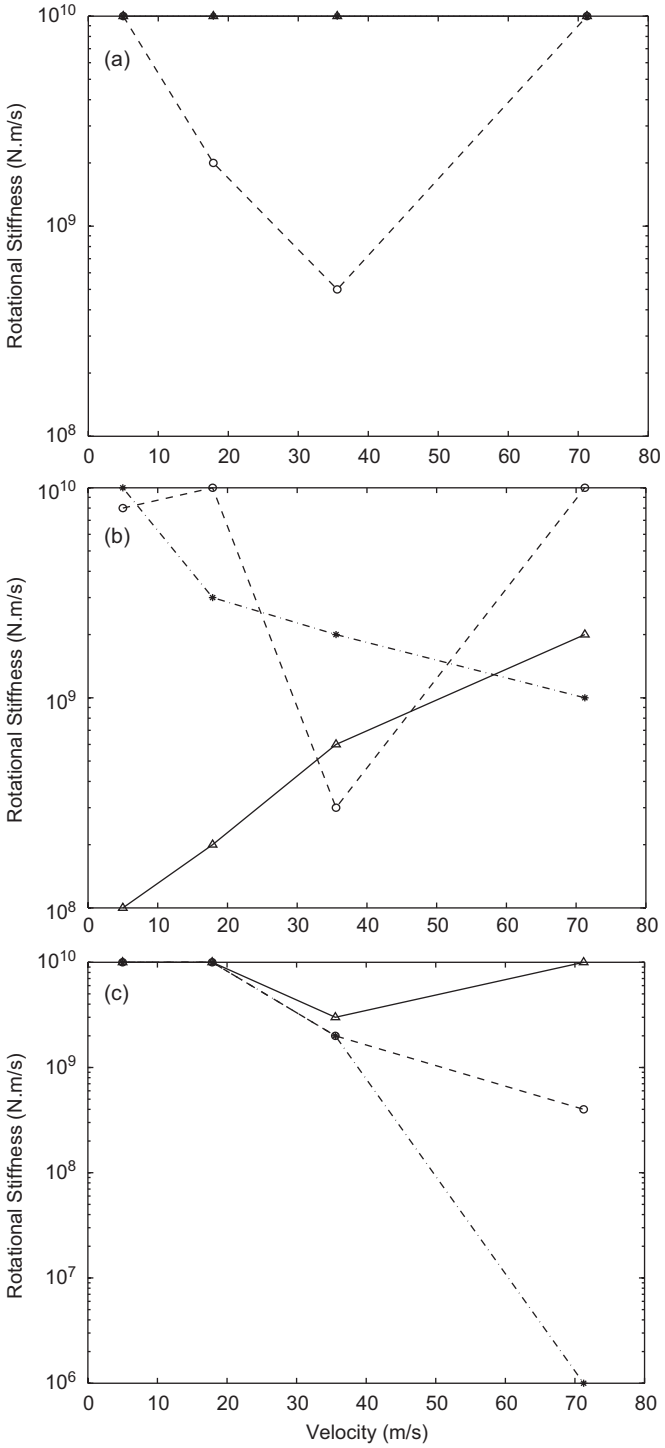

Fig. 13. The rotational coupling stiffness that corresponds to the smallest peak–peak deflection at the midpoint of each span for a constant acceleration $a = 2\,\mathrm{m/s^2}$: (a) span 1; (b) span 2; and (c) span 3. (—△—) Elastic–elastic; (- -⊖- -) rigid–elastic; and (—✻—) elastic–rigid.

degenerate into a continuous multi-span beam, and the responses tend to become the same as repeatedly shown in Figs. 9–11.

The above results have consistently indicated that the dynamic behavior of a multi-span bridge may become strongly dependent upon the coupling conditions between spans. Since in practice the stiffness values can vary easily by several orders of magnitude, their impact on the dynamic behavior will be better assessed in terms of the variance ratio, as plotted in Fig. 12. The variance ratio is defined as the deference between the maximum and minimum peak–peak deflections (normalized by the maximum) for all the given stiffness values. A larger variance ratio indicates a more significant influence of the coupling conditions on the dynamic behavior of the bridge. It is evident from Fig. 12 that the deflections or the dynamic behavior of a bridge can be substantially influenced by the coupling conditions.

In terms of bridge design, a large variance ratio implies certain room for improving bridge performance through varying or optimizing the coupling conditions between spans. For example, a set of preferred joint stiffnesses (corresponding to the minimum peak–peak deflection) are shown in Fig. 13 for the specified load speeds. It is clear that the rigid coupling does not always result in the smallest deflection, as one may intuitively believe. It should be pointed out that these optimal stiffness values were actually determined based on the local vibration data and vary from span to span. In practice, one may have to first define a global objective or cost function so that a unique set of optimal joint parameters can be found accordingly. Since the coupling conditions, unlike many other structural parameters, can be modified in a more drastic and cost-effective manner, they have potential to become an important design option for a significant improvement of bridge performance.

4. Conclusions

The vibration of a multi-span bridge subjected to a moving load has been investigated in a generic manner. Unlike in most previous multi-span bridge models, the displacement and its derivative are not here required to be continuous at the intermediate supports or any other locations. In other words, the joints between spans can be considered as the design variables and optimized to achieve desired performance. In essence, the current model is a more general representation of multi-span bridges in that each span can be independently supported and arbitrarily coupled to its neighbors via a set of joints of any stiffness values.

Since the traditional beam and material parameters have been extensively studied and well understood regarding their effect on the bridge vibration, this investigation is specifically focused on a set of rarely attempted model variables: the coupling conditions between spans. It has been demonstrated through numerical examples that the coupling conditions will generally have a direct and meaningful impact on the vibration on each span. In particular, the peak–peak deflection on a span is strongly dependent upon the coupling conditions local to that span, and less sensitive to the coupling conditions at distant junctions. For a given coupling arrangement, the peak–peak deflection on each span typically increases with the traveling speed of a load. In comparison with many other design variables, a coupling stiffness can be practically varied easily by several orders of magnitude. It is found, however, that the dynamic behavior becomes particularly sensitive to the coupling conditions near the critical stiffness value defined by $KL/EI \cong 1$. Thus, the large design space may be practically compressed into a much smaller one. Finally, a large variance ratio for the deflection on each span shall be understood as a good potential for improving bridge design through optimizing the coupling conditions between spans. In the current model, there are up to eight independent (supporting and coupling) springs associated with each span. While this model generalization may appear to complicate a design task, it actually opens more avenues for significantly improving or modifying the dynamic behavior of a multi-span bridge.

Acknowledgment

This research is supported by NSF Grant CMS-0528263 under the supervision of Dr. Eduardo Misawa.

References

[1] J. Hino, T. Yoshimura, N. Ananthanarayana, A finite element method prediction of the vibration of a bridge subjected to a moving vehicle load, *Journal of Sound and Vibration* 96 (1) (1984) 45–53.

[2] M. Olsson, Finite element, modal co-ordinate analysis of structures subjected to moving loads, *Journal of Sound and Vibration* 99 (1) (1985) 1–12.

[3] Y.H. Lin, M.W. Trethewey, Finite element analysis of elastic beams subjected to moving dynamic loads, *Journal of Sound and Vibration* 136 (2) (1990) 323–342.

[4] K. Henchi, M. Fafard, Dynamic behavior of multi-span beams under moving loads, *Journal of Sound and Vibration* 199 (1) (1997) 33–50.

[5] R.T. Wang, J.S. Lin, Vibration of multi-span Timoshenko frames due to a moving load, *Journal of Sound and Vibration* 212 (3) (1998) 417–434.

[6] R.T. Wang, T.Y. Lin, Random vibration of multi-span Timoshenko beam due to a moving load, *Journal of Sound and Vibration* 213 (1) (1998) 127–138.

[7] Y.A. Dugush, M. Eisenberger, Vibrations of non-uniform continuous beams under moving loads, *Journal of Sound and Vibration* 254 (5) (2002) 911–926.

[8] H.P. Lee, Dynamic response of a beam with intermediate point constraints subject to a moving load, *Journal of Sound and Vibration* 171 (3) (1994) 361–368.

[9] Y. Cai, S.S. Chen, D.M. Rote, H.T. Coffey, Vehicle/guideway interaction for high-speed vehicles on a flexible guideway, *Journal of Sound and Vibration* 175 (5) (1994) 625–646.

[10] H.P. Lee, Transverse vibration of a Timoshenko beam acted upon by an accelerating mass, *Applied Acoustics* 47 (4) (1996) 319–330.

[11] P.D. Cha, A general approach to formulating the frequency equations for a beam carrying miscellaneous attachments, *Journal of Sound and Vibration* 286 (4–5) (2005) 921–939.

[12] M. Ichikawa, Y. Miyakawa, Vibration analysis of the continuous beam subjected to a moving mass, *Journal of Sound and Vibration* 230 (3) (2000) 493–506.

[13] D.Y. Zheng, Y.K. Cheung, F.T.K. Au, Y.S. Cheng, Vibration of multi-span non-uniform beams under moving loads by using modified beam vibration functions, *Journal of Sound and Vibration* 212 (3) (1998) 455–467.

[14] Y.K. Cheung, F.T.K. Au, D.Y. Zheng, Y.S. Cheng, Vibration of multi-span non-uniform bridges under moving vehicles and trains by using modified beam vibration functions, *Journal of Sound and Vibration* 228 (3) (1999) 611–628.

[15] R. Hamada, Dynamic analysis of a beam under a moving force: a double Laplace transform solution, *Journal of Sound and Vibration* 74 (2) (1981) 221–233.

[16] R.P. Goel, Free vibrations of a beam-mass system with elastically restrained ends, *Journal of Sound and Vibration* 47 (1) (1976) 9–14.

[17] S.-W. Hong, J.-W. Kim, Modal analysis of multi-span Timoshenko beams connected or supported by resilient joints with damping, *Journal of Sound and Vibration* 227 (4) (1999) 787–806.

[18] T.P. Chang, F.I. Chang, M.F. Liu, On the eigenvalues of a viscously damped simple beam carrying point masses and springs, *Journal of Sound and Vibration* 240 (4) (2001) 769–778.

[19] E.H. Dowell, On some general properties of combined dynamical systems, *Journal of Applied Mechanics* 46 (1) (1979) 206–209.

[20] M. Gürgöze, On the alternative formulations of the frequency equation of a Bernoulli–Euler beam to which several spring-mass systems are attached in-span, *Journal of Sound and Vibration* 217 (2) (1998) 585–595.

[21] B. Posiadała, Free vibrations of uniform Timoshenko beams with attachments, *Journal of Sound and Vibration* 204 (2) (1997) 359–369.

[22] J.W. Nicholson, L.A. Bergman, Free vibration of combined dynamical systems, *Journal of Engineering Mechanics* 112 (1) (1986) 1–13.

[23] L.A. Bergman, D.M. McFarland, On the vibration of a point-supported linear distributed system, *ASME Journal of Vibration, Acoustics, Stress, and Reliability in Design* 110 (4) (1988) 485–592.

[24] M. Abu-Hilal, Forced vibration of Euler–Bernoulli beams by means of dynamic Green functions, *Journal of Sound and Vibration* 267 (2) (2003) 191–207.

[25] S. Kukla, Application of Green functions in frequency analysis of Timoshenko beams with oscillators, *Journal of Sound and Vibration* 205 (3) (1997) 355–363.

[26] M.A. Foda, Z. Abduljabbar, A dynamic Green function formulation for the response of a beam structure to a moving mass, *Journal of Sound and Vibration* 210 (3) (1998) 295–306.

[27] Y.B. Yang, C.L. Lin, J.D. Yau, D.W. Chang, Mechanism of resonance and cancellation for train-induced vibrations on bridges with elastic bearings, *Journal of Sound and Vibration* 269 (1–2) (2004) 345–360.

[28] J.D. Yau, Y.S. Wu, Y.B. Yang, Impact response of bridges with elastic bearings to moving loads, *Journal of Sound and Vibration* 248 (1) (2001) 9–30.

[29] Y. Chen, C.A. Tan, L.A. Bergman, Effects of boundary flexibility on the vibration of a continuum with a moving oscillator, *ASME Journal of Vibration and Acoustics* 124 (4) (2002) 552–560.

[30] W.L. Li, Free vibrations of beams with general boundary conditions, *Journal of Sound and Vibration* 237 (4) (2000) 709–725.

[31] W.L. Li, M.W. Bonilha, J. Xiao, Vibrations and power flow in a coupled beam system, *Journal of Vibration and Acoustics* 129 (5) (2007) 616–621.

[32] W.L. Li, M.W. Bonilha, J. Xiao, Prediction of the vibrations and power flows between two beams connected at an arbitrarily angle, *Proceedings of the SAE Noise and Vibration Conference*, Traverse City, MI, 05NVC-222, 2005.

[33] W.L. Li, Hongan Xu, A general Fourier series method for the vibration analysis of multi-span beam systems. *Journal of Computational and Nonlinear Dynamics*, submitted for publication.